

Evaluation of a wind power parameterization using tower observations

Steven M. Lazarus and Jennifer Bewley

Department of Marine and Environmental Systems, Florida Institute of Technology, Melbourne, Florida, USA

Received 17 November 2004; revised 30 November 2004; accepted 6 January 2005; published 6 April 2005.

[1] The spatial and temporal components of a published wind power parameterization method are evaluated using observed winds (9 m to 90 m) from 7 years of data collected at four towers in the Kennedy Space Center/Cape Canaveral Air Force Station network. The temporal component is governed by two parameterization inputs which represent the amplitude and mean of an assumed sinusoidal diurnal variation of the ratio of the 80 m to 10 m winds, respectively. Comparison with tower observations shows that the estimates of the mean ratio are robust but biased high, indicating that the temporal variation of the observations can be approximated by, but is not, a pure sinusoid. The observed and parameterized amplitude are poorly correlated as the amplitude estimate is sensitive to small phase shifts in the diurnal variation of the ratio of the wind speeds. The observed annual wind power for the site is consistent with what is known about the wind energy potential in Florida, while wind power estimates based on the temporal extrapolation are more than twice that observed. The erroneous wind power estimate is shown to be related to an assumption that negative amplitude estimates are indicative of a diurnal phase shift in the ratio of the 80 m to 10 m winds. When the assumed phase shift is removed from the data and the observed inputs are applied, the parameterized 80 m wind power estimates were comparable to those observed. The spatial component of the parameterization depends on a least squares fit of four different wind extrapolation methods to 0000 and 1200 UTC wind profiles. Comparison of the observed 80 m winds with those obtained via the least squares method indicates that the 0000 UTC 80 m wind and power estimates exceed (by as much as 1 m s^{-1} and 200 W m^{-2} , respectively) the observed 80 m winds and power for all months. When compared against the 0000 UTC regression, the 1200 UTC 80 m wind and power estimates are closer to the observed power for all months. The power law often yields the lowest residual (on the order of 15–20% of the time) but is also largely responsible for high power estimates. The positive power bias (i.e., estimated greater than observed) is a result of the combination of two factors, namely, (1) the 0000/1200 UTC profiles and 10 m winds are, in general, not representative of the daily averaged values, with the 0000 and 1200 UTC 10 m winds less than their daily average, and (2) the differences between the observed 80 m and 10 m 0000 and 1200 UTC winds are greater than the difference between the daily averaged 80 m and 10 m mean winds. These results illustrate the potentially problematic nature of combining the lowest residual producing (extrapolation) method, obtained from a fit to the 0000 or 1200 UTC wind profiles, and the daily-averaged 10 m wind to produce a daily-averaged 80 m wind estimate.

Citation: Lazarus, S. M., and J. Bewley (2005), Evaluation of a wind power parameterization using tower observations, *J. Geophys. Res.*, 110, D07102, doi:10.1029/2004JD005614.

1. Introduction

[2] Various methods have been applied in attempt to quantify “regional” wind power. While the motivation is clear, i.e., to provide a basis upon which critical decisions regarding the siting of wind energy farms can be made, the techniques used to map regional wind resources remain only

marginally useful in that they are not designed to identify variability on a local scale and hence do not circumvent the need for site-specific wind measurement efforts. This is especially the case in complex terrain or in coastal regions where there can be significant differences between offshore and onshore wind resources [e.g., *Brower, 2002*].

[3] Wind resource mapping and surveys have been conducted in the past [e.g., *Petersen et al., 1981; Elliott et al., 1986; Troen and Petersen, 1989; Schwartz and Elliot, 2001*] with current techniques tending toward high-resolu-

tion mesoscale modeling systems that act as a surrogate to observations, i.e., produce the wind climatology. The advantage of such systems is that they can simulate complex meteorological phenomena (e.g., sea breeze, slope flows, nocturnal jets, boundary layer evolution and decoupling, surface roughness, etc.) that are not represented in wind flow models or impractical to observe at similar resolutions over a large region. Despite the benefits of modeling a wind climatology, the models have limitations, some of which are often accentuated at high resolution. For example, the model physics, e.g., radiation, turbulence, microphysics, which are parameterized (to varying degrees), are particularly relevant for producing realistic high-resolution simulations (i.e., they must accurately represent the submesoscale or local forcing especially for relatively quiescent large-scale conditions, e.g., slope/drainage flows in complex terrain).

[4] In the absence of model data or turbine-level observations, it is common practice to extrapolate surface wind data upward to produce and evaluate wind map climatologies. For example, the National Renewable Energy Laboratory (NREL) national wind energy atlas wind resource analysis was composited using data primarily collected at heights ranging 3 to 15 m agl, with extrapolation to higher levels based on the 1/7 power law. The power law [Elliott *et al.*, 1986] and logarithmic law [Arya, 1988] have well-known limitations yet are frequently used because of their simple nature. Recent work by Archer and Jacobson [2003] (hereinafter referred to as AJ) applies both of these commonly used profiles to a least squares methodology and a combination of surface observations and radiosonde data. In their work they “best fit” the winds from multiple upper air stations with the winds (10 m) from a single surface station to obtain an estimate of the 80 m wind at the surface station in question. For 10 of their surface stations in which hourly data are available, the 80 m wind speeds are also interpolated in time to fill the gaps between the sonde times (typically 0000 and 1200 UTC).

[5] The AJ results were somewhat surprising in that they show relatively significant wind energy potential at a few sites along the Florida east coast [e.g., Archer and Jacobson, 2003, Figure 3], an area regarded by previous studies to have insufficient winds [e.g., Elliott *et al.*, 1986]. Various aspects and assumptions of the AJ technique are examined by comparing their methodology to high-resolution wind tower data collected at the Kennedy Space Center over a 7 year period.

2. Data

[6] Five-minute data (1995–2001) from the meteorological tower data network at the Kennedy Space Center (KSC) and Cape Canaveral Air Station (CCAS) are used to produce the statistics for this work. The wind speed and direction were sampled at 1-s resolution and then averaged to create a time series of 5-min means. The data were processed for errors using a sequence of checks including unrealistic values, standard deviation, a peak-to-average wind speed ratio, and vertical/temporal consistency [Lambert, 2002]. The KSC tower network is extensive, with 48 independent towers 4 of which have redundant sensors. Of the 48 towers, 4 measure winds at levels above 200 feet (62 m). Data from KSC tower number 3131 (for location, see Figure 1), which

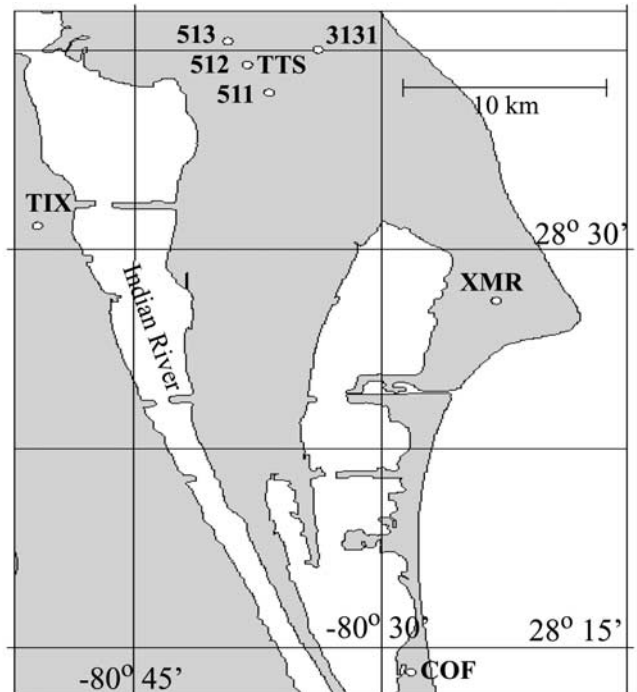


Figure 1. Tower and surface data locations (see Table 2 for more information). Map obtained from Online Map Creation (http://www.aquarius.geomar.de/omc/omc_intro.html) and Wessel and Smith [1995].

has sensors mounted at 1.8 m, 3.7 m, 16.5 m, 49.4 m, 62.2 m, 89.9 m, 120.1 m, and 150 m, are used in validating against the turbine level winds (wind turbines in the megawatt range have towers of 60 to 100 m). At each level, tower 3131 has two sensors mounted on the northeast and southwest sides of the tower. Data from three nearby towers in the network (tower 511, 512, and 513) each of which have 9 m winds (tower 3131 has 3.7 m and 16.5 m winds but does not have 9 m winds), are also used herein.

[7] With the exception of last 6 months of 2000, the data availability for the 7 year period is generally quite good and ranges from a low near 70% in January (for all levels) to more than 95% for the month of March. Data prior to 29 January 1995 were removed (in entirety) from the data stream as it marked the end of a period where KSC/CCAS transitioned from a less accurate measuring system.

3. Method

3.1. Archer and Jacobson

[8] The AJ least squares (LS) estimate of the 80 m wind (V80) is produced by pairing 5 proximity soundings with the 10 m wind (V10) at a single surface station. In their method they regress the sounding winds (at three levels) against both the power law and logarithmic law, choosing the fit with the lowest residual to reproduce the empirical wind profile at each of the sounding locations. For cases where the wind speed decreases with height, AJ linearly extrapolate upward (from 10 m) to 80 m in order to avoid producing spuriously large 80 m winds. These profiles are then fit to the 10 m wind observations at the individual stations to produce an “estimate” of the 80 m winds at each

Table 1. The 80 m Wind Speeds and Corresponding Wind Power Class

Class	80 m Wind Speed, m s ⁻¹
1	0.0–5.9
2	5.9–6.9
3	6.9–7.5
4	7.5–8.1
5	8.1–8.6
6	8.6–9.4
7	>9.4

of the 5 sounding stations. It is this estimate that is interpolated (via inverse distance weighting) back to the station locations to produce an 80 m wind estimate valid at the sonde times (i.e., 0000 and 1200 UTC).

[9] Because the soundings, and hence estimates of V80, are generally limited to 0000 and 1200 UTC, AJ use the ratio of the 80 m to 10 m winds ρ calculated at the sounding times to fill in the hourly V80 trends at the station. For 10 of their stations in which the hourly 10 m wind data were available, the AJ V80 trend is modeled as a sinusoid,

$$\rho(h) = A \times \sin\left[(h - \delta) \frac{\pi}{12}\right] + \bar{\rho} \quad (1)$$

where $A = 0.5*(\rho_{\max} - \rho_{\min})$, h is the time of day (UTC), δ is the time shift (hours) that ensures that the sinusoid minimum in ρ matches the observed ρ_{\min} , and $\bar{\rho}$ is the diurnal mean V80 to V10 ratio. Because AJ do NOT have $\bar{\rho}$, they apply/assume the following:

$$\bar{\rho} = \frac{0.95 \times (\rho_{00} + \rho_{12})}{2} \quad (2)$$

where ρ_{00} and ρ_{12} are 0000 and 1200 UTC ratio of V80 to V10 winds respectively and the denominator was obtained such that the AJ $\bar{\rho}$ (hereafter $\bar{\rho}_{AJ}$) estimate matched an observed $\bar{\rho}$ based on a 6-year PNL data set from 16 sites [Sandusky *et al.*, 1982].

[10] To estimate the amplitude A (hereafter A_{AJ}) of the sinusoid in equation (1) above AJ also make the following approximation

$$A = \frac{\alpha(\rho_{12} - \rho_{00})}{2} \quad (3)$$

where by trial and error they pick $\alpha = 1.2$. There may be days where $\rho_{12} < \rho_{00}$ which produces a negative amplitude. It is not obvious how to deal with these days. For example, one can (1) remove all days for which $A_{AJ} < 0$, (2) take the absolute value of A_{AJ} , or (3) allow the amplitude to be negative (option 3 results in a 12 h phase shift in $\rho(h)$). AJ assume the latter of the three and, without 80 m wind data, it is impossible to evaluate the validity of their assumption (C. L. Archer, personal communication, 2004).

[11] In order to eliminate negative wind speeds, AJ remove days where $|A_{AJ}| > \bar{\rho}_{AJ}$ which, in our data stream represents less than 3% of the total data depending on the month (see Table 3). Note however, that removing days where the amplitude is large may bias the wind power estimates low. It is also not clear whether or not the sinusoidal fit is appropriate for this site (e.g., a collapse in

the daytime mixed layer may produce significant asymmetries in the observed diurnal cycle of ρ). These latter two issues are revisited in more detail in section 4.

[12] The aforementioned temporal issues are not relevant with respect to AJ's Figure 3 (wind map) because hourly data were not available at many of the surface stations. As a result, the AJ wind map is produced using a combination of their LS methodology and daily-averaged values for V10 at each individual surface station. If two soundings are available on a given day, an average of the 80 m wind obtained from each profile is used. Both AJ approaches are used/evaluated herein to estimate the 80 m wind power in a small region along the central Florida coast near the Kennedy Space Center.

[13] The NREL-based wind power class rating system for 80 m winds is given in Table 1, while AJ wind power class estimates for several sites and their elevations in the region of interest are given in Table 2. All sites are associated with airport runways except for the TTS site which is a NASA shuttle facility landing pad. The stations include one mainland station, TIX (adjacent to the Indian River Lagoon (IRL)), and three barrier island stations: XMR, COF, and TTS. The AJ wind power class estimates for these sites are 2 at TTS and 1 at XMR, and 7 at both COF and TIX. Because of the relative proximity of these stations, the AJ method pairs each with the same five proximity sounding locations (Tampa Bay, TBW; Kennedy Space Center, XMR; Jacksonville, JAX; Miami, MFL; and Key West, EYW; see Figure 2). XMR is the closest (and thus most heavily weighted) upper air station to all 4 of these surface stations followed by TBW.

[14] The order in which the upper air stations are weighted differs only slightly between that of COF and XMR and is identical between TTS and TIX (Archer, personal communication, 2004). Also, each of the sites under consideration, including the tower data, are situated in a relatively open space along runways in areas that are of similar surface roughness. Hence the striking difference in AJ power

Table 2. Central East Coast Florida Station Locations and Upper Air 80 m Wind Speeds (V80) and 80 m Wind Power Class for the Year 2000^a

Station	Location	Latitude, deg	Longitude, deg	V80	AJ Class
TTS	NASA shuttle facility (3.1 m)	28.6160	-80.6930	6.79	2
COF	Patrick AFB/Cocoa Beach (2.4 m)	28.2349	-80.6101	10.25	7
XMR	Cape Kennedy (AFS, 3.1 m)	28.4677	-80.5668	5.72	1
TIX	Titusville (10.4 m)	28.5148	-80.7992	9.53	7
MFL	Miami International (4 m)	25.75	-80.38	4.50	1
JAX	Jacksonville International (9 m)	30.43	-81.70	4.89	1
TBW	Tampa International	27.70	-82.40	4.29	1
TLH	Tallahassee Regional 21 m	30.38	-84.37	3.85	1
3131	KSC Tower 3131	28.6256	-80.6571	5.80	1
0511	KSC Tower 511	28.5986	-80.6817		
0512	KSC Tower 512	28.6160	-80.6930		
0513	KSC Tower 513	28.6308	-80.7027		

^aAlso shown are the Kennedy Space Center tower locations. Station elevation (m ASL) is given in parentheses. The 80 m wind power class data are provided by Archer and Jacobson [2003].

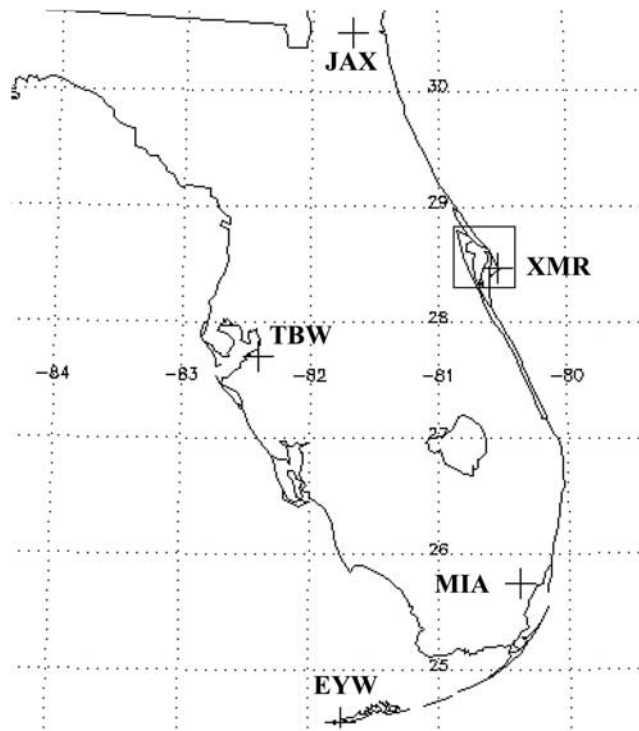


Figure 2. Upper air locations. Box indicates approximate area shown in Figure 1.

estimates between these proximity stations is likely related to the 10 m winds at these locations. It is also interesting to point out that the AJ 80 m wind power class at each of the sonde locations shown in Figure 2 is 1, each with average annual 80 m winds $<5.9 \text{ m s}^{-1}$ (Table 2).

3.2. Observations

[15] Here the AJ parameters are calculated directly and compared to observations. For example, the ratio of the V80 to V10 wind speeds are calculated at the 5 min. resolution of the data. Because the tall tower (3131) does not have 9 m winds, a combination of the 90 m level winds from tower 3131 and 9 m winds from three nearby towers (511, 512, and 513 see Figure 1) are used. The brackets included in Tables 3 and 4 are the minimum and maximum values obtained from 3 distinct estimates calculated from the pairing of the 9 m data from towers 511, 512, and 513 and the 90 m data from tower 3131. The AJ parameters are then compared with their observed counterparts (i.e., “truth”) from which their impact on the wind energy estimates at the KSC can be evaluated.

[16] The daily amplitude is calculated assuming a fixed value for δ which is taken to be zero for all months (note here we define ρ to be a function of time in UTC not LST as in AJ). With δ fixed, a least squares fit for the mean and amplitude in equation (1) above is performed. This yields two equations and two unknowns (A , $\bar{\rho}$),

$$\begin{bmatrix} \bar{\beta}^2 & \bar{\beta} \\ \bar{\beta} & 1 \end{bmatrix} \begin{bmatrix} A \\ \bar{\rho} \end{bmatrix} = \begin{bmatrix} \overline{\rho^{obs}\beta} \\ \overline{\rho^{obs}} \end{bmatrix} \quad (4)$$

where $\beta = \sin(\pi h/12)$. Here, $\bar{\beta} = 0$ and hence $\bar{\rho} = \overline{\rho^{obs}}$ and $A = \overline{\rho^{obs}\beta}/\bar{\beta}^2$.

4. Temporal Evaluation

[17] Using daily inputs, the monthly averages of the observed and AJ A and $\bar{\rho}$ are calculated. The statistics for each pairing of the 9 m tower winds (511, 512, and 513) with the tall tower (3131) 90 m winds are shown in Table 4. For all months and towers, A_{AJ} is smaller than the observed amplitude A . Except for summer months (May–August), $\bar{\rho}_{AJ}$ is greater than $\bar{\rho}$. As one might expect for the region, the observed magnitudes of both parameters are maximum (minimum) in the cool (warm) season.

[18] Because the wind power potential varies as the cube of the wind speed it is advantageous to examine its sensitivity to the AJ parameters (A and $\bar{\rho}$). Using equation (1) one can express the wind power in terms of the AJ parameterization, i.e.,

$$P(h, A, \bar{\rho}) = \frac{1}{2} \rho_{air} V_{10}^3(h) \left[A \sin\left(\frac{\pi h}{12}\right) + \bar{\rho} \right]^3 \quad (5)$$

where ρ_{air} is the air density (taken to be 1.225 kg m^{-3}), and V_{10} is the 10 m wind speed (the actual power yield from a large turbine however is more closely related to a square relationship as it involves a combination of equation (5) and the actual wind distribution). Despite the finding that, in general, $\bar{\rho}_{AJ}$ is greater than $\bar{\rho}$ while A_{AJ} is less than A (the net effect would tend to cancel one another in terms of their impact on the AJ 80 m wind power estimate, e.g., Figure 3), the AJ method significantly overestimates the 80 m power (Table 4) when compared to the observations, yielding estimates well above that observed for all months.

4.1. Bias and Nonlinearity

[19] As with all nonlinear parameterizations, the estimate of a nonlinear function value using the average of the inputs will not equal the average of the function calculated using the individual inputs [e.g., Larson et al., 2001]. The sensitivity of the AJ parameterization using representative

Table 3. Percentage of Observed 80 m Winds (V80) Less Than the 10 m Wind Speeds (V10), Percentage of AJ Amplitudes A_{AJ} That are Greater Than the AJ Estimate of the Ratio of the 80 m to 10 m Winds ρ_{AJ} , and Percentage A_{AJ} Less Than Zero^a

Month	Percent V80 < V10	Percent Observed $ A_{AJ} > \bar{\rho}_{AJ}$	Percent Observed $A_{AJ} < 0$
January	[4.5, 4.9]	[0.0, 0.7]	[42.9, 50.7]
February	[5.7, 6.3]	0.0	[31.1, 37.7]
March	[5.6, 6.7]	0.0	[34.8, 39.1]
April	[5.9, 6.3]	0.5	[30.4, 35.1]
May	[7.5, 7.6]	1.0	[45.6, 52.5]
June	[9.4, 10.1]	[2.8, 3.2]	[51.7, 55.4]
July	[14.2, 14.8]	0.6	[43.6, 48.6]
August	[9.0, 9.6]	[1.3, 1.7]	[44.9, 47.0]
September	[6.7, 7.2]	[1.3, 2.0]	[42.4, 44.6]
October	[3.7, 4.3]	[0.6, 1.8]	[42.1, 53.8]
November	[4.0, 4.6]	[0.7, 1.3]	[45.6, 52.8]
December	[5.0, 5.4]	[0.6, 1.0]	[43.8, 53.3]

^aBrackets represent the minimum and maximum values calculated using the 9 m winds from towers 511, 512, and 513. Refer to equation (3) for A_{AJ} and to equation (2) for ρ_{AJ} .

Table 4. Observed and Estimated Amplitude A, 80 m Winds V80, 80 m to 10 m Wind Ratio $\bar{\rho}$, and Wind Power P for the Pairing of 9 m Winds From Towers 511, 512, and 513 and 90 m Winds From Tower 3131^a

Month	A	A _{AJ}	V80, m s ⁻¹	V80 _{AJ} , m s ⁻¹	$\bar{\rho}$	$\bar{\rho}_{AJ}$	P, W m ⁻²	P _{AJ} , W m ⁻²	P _{AO} , W m ⁻²
January	[0.94, 0.96]	[0.65, 0.71]	6.5	[8.2, 8.6]	[2.26, 2.30]	[2.46, 2.60]	252	[862, 1026]	253
February	[0.92, 1.03]	[0.71, 0.76]	6.5	[8.4, 8.5]	[2.18, 2.25]	[2.44, 2.57]	265	[945, 970]	353
March	[0.83, 0.87]	[0.59, 0.67]	6.6	[8.2, 8.5]	[2.00, 2.05]	[2.21, 2.32]	273	[702, 907]	346
April	[0.94, 0.96]	[0.62, 0.77]	6.2	[7.5, 7.9]	[2.03, 2.08]	[2.18, 2.35]	202	[528, 739]	277
May	[0.90, 0.97]	[0.47, 0.51]	5.4	[6.1, 6.3]	[1.93, 2.05]	[1.89, 2.02]	133	[338, 372]	175
June	[0.75, 0.83]	[0.49, 0.54]	4.9	[5.3, 5.5]	[1.87, 1.96]	[1.74, 1.82]	112	[261, 486]	138
July	[0.80, 0.88]	[0.47, 0.57]	4.6	[5.0, 5.4]	[1.85, 1.97]	[1.72, 1.98]	84	[230, 340]	105
August	[0.77, 0.88]	[0.59, 0.66]	4.6	[5.6, 5.9]	[1.92, 2.06]	[2.06, 2.21]	120	[336, 400]	124
September	[0.81, 0.90]	[0.60, 0.63]	4.9	[6.2, 6.4]	[2.05, 2.14]	[2.26, 2.34]	145	[420, 460]	168
October	[0.81, 0.88]	[0.54, 0.64]	6.4	[7.9, 8.0]	[2.12, 2.20]	[2.42, 2.48]	267	[646, 776]	287
November	[0.98, 0.99]	[0.71, 0.82]	6.3	[8.3, 8.6]	[2.31, 2.36]	[2.63, 2.76]	233	[922, 1590]	216
December	[0.99, 1.09]	[0.76, 0.80]	6.0	[7.6, 7.9]	[2.30, 2.47]	[2.51, 2.75]	190	[984, 1744]	270
Average			5.8	7.1, 7.3					

^aThe subscripts “AJ” and “AO” indicate estimate using the AJ methodology and the AJ methodology with observed A and ρ , respectively (assuming A is always greater than zero). Brackets represent the minimum and maximum values calculated using the 9 m winds from towers 511, 512, and 513.

observed values for the inputs A (=0.85) and $\bar{\rho}$ (=2.0) is examined in order to gauge the potential for using an extended average (e.g., monthly) of the AJ inputs to estimate the wind power. Here “representative” implies a selection of reasonable (i.e., within the bounds of those observed) parameter values from Table 4. Figures 3a and 3b indicate that both curves are concave up and, as a result, suggest that wind power estimates using an average (e.g., monthly) of the Archer input parameters (which lie on the

parabola for the given value of the average input) will underestimate (erroneously) the wind power when compared to the average power calculated for individual input values (e.g., for two inputs this lies at the midpoint on a straight line connecting the two points). Of particular note, the AJ parameterization is only weakly nonlinear with respect to the amplitude (for observed A ranging from 0 to 1 in Figure 3a). For the observed ranges of the average monthly parameters, the AJ parameterization exhibits greater range in the wind power estimate due to variations in $\bar{\rho}$ (~ 250 W m⁻²) than due to variations in A (~ 50 W m⁻²).

[20] In order to examine the impact of the AJ parameters on the estimated power, a plot of $\bar{\rho}$ versus $\bar{\rho}_{AJ}$ for each individual day for the month of January (for all years) is shown (Figure 4). The observed and AJ estimates are fairly

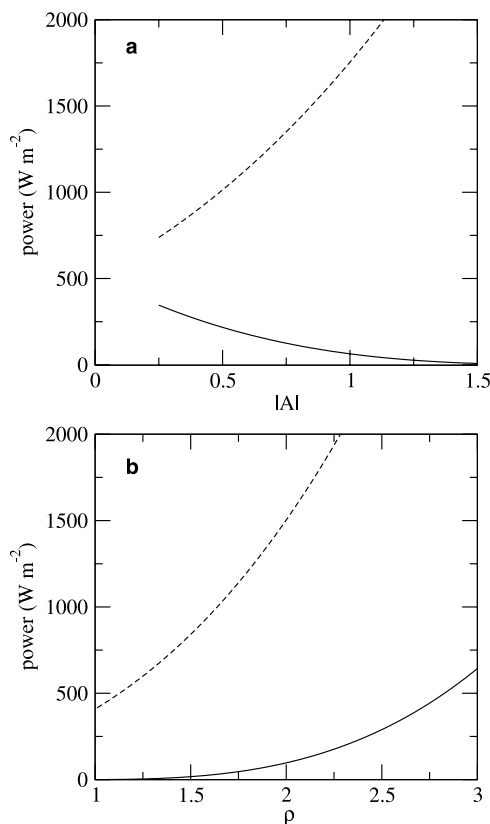


Figure 3. Power (W m⁻²) versus (a) the absolute value of the amplitude, A, using a representative (and fixed) value of $\bar{\rho}$ (=2.0), and (b) the average ratio of the 80 m to 10 m winds, $\bar{\rho}$, for A = 0.85. Dashed curves are for negative amplitudes.

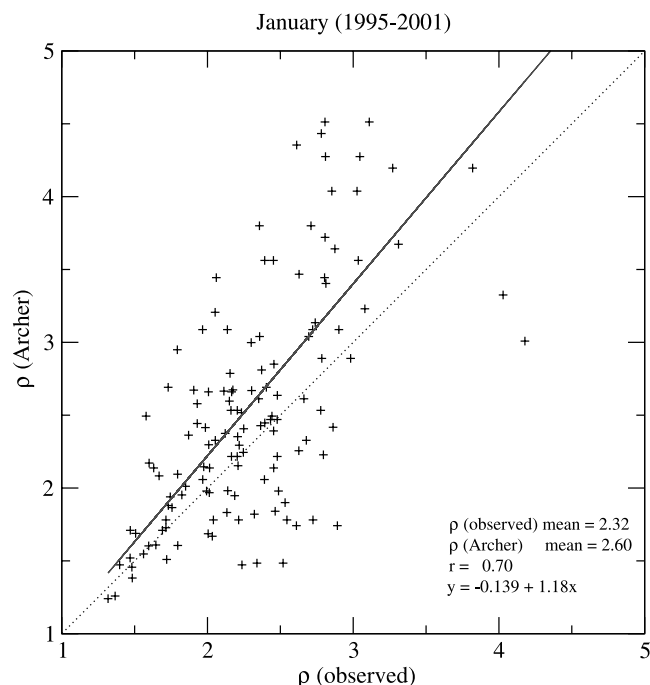


Figure 4. Daily $\bar{\rho}$ estimates from AJ (equation (2)) versus the observed for the month of January (all years). The dotted line is the one-to-one curve, and the solid line is a least squares fit.

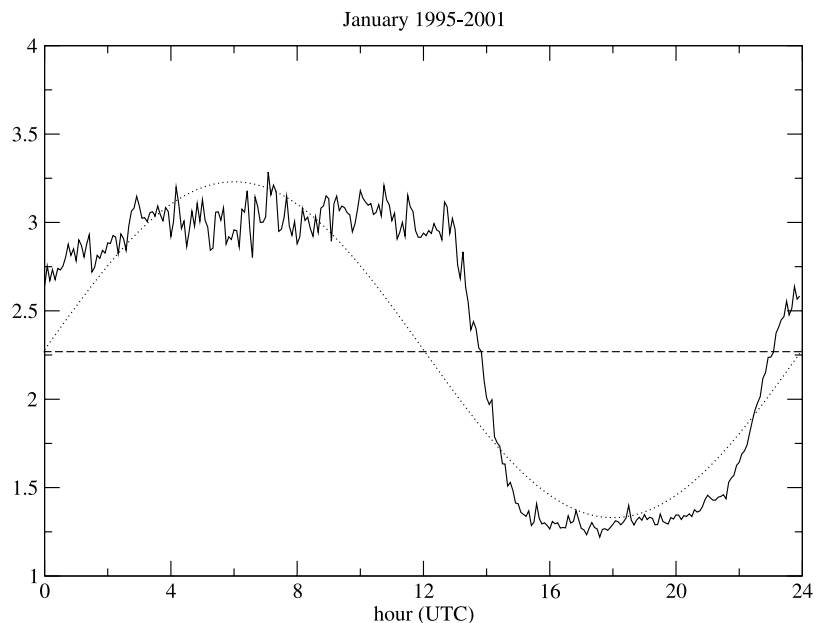


Figure 5. Observed ρ time series for January. Individual 5 min observations were averaged over all years (1995–2001). Monthly mean observed ($\bar{\rho}$) is given by the dashed line, and the observed sinusoidal fit (using $\bar{\rho}$ and A from Table 4) is given by the dotted line.

well correlated and the slope of the curve ~ 1.2 suggests that the $\bar{\rho}_{AJ}$ estimate is robust but biased high. The high bias can be explained simply by considering the observed January $\rho(h)$ time series (Figure 5). Because the observed time series is not a pure sinusoid, $\bar{\rho}$ for the month of January (dashed line) is clearly less than $\bar{\rho}_{AJ}$ (Table 4) which uses ρ_{00} and ρ_{12} only. Similarly, A and A_{AJ} are compared (Figure 6, where A is the absolute value of AJ estimate from equation (3)). In contrast to $\bar{\rho}$, the observed and parameterized amplitude is poorly correlated suggesting that the AJ estimate of the amplitude is not robust. This is not surprising as an estimate of an amplitude using only two points will likely be quite variable because of its dependence on small phase shifts in the diurnal signal. This is not the case for $\bar{\rho}$ estimates where, for a pure sinusoid, the average of any two samples 12 h apart will always yield the mean.

4.2. Evaluation of Parameterization Assumptions

[21] AJ estimates of 80 m wind power depend on the cube of both $\bar{\rho}$ and A , and it was mentioned previously that values, of these parameters, larger than observed will contribute to spuriously large power estimates. However, as previously discussed, both $\bar{\rho}_{AJ}$ and A_{AJ} are such that, in tandem, their impact on the AJ 80 m wind power estimate would be minimal, both less than observed (Table 4). Additionally, AJ power estimates for a wide range of input parameter values (Figure 3) are generally less than 500 W m^{-2} which, for most months, are substantially smaller than the AJ values shown in Table 4 and hence are not likely the cause of the overestimate of the AJ wind power here. In an effort to identify the source for the spurious power estimates, various observed statistics are presented in Table 3. For the most part, the wind speed increases with height, with the exception of summer months (June–August) when the sea breeze circulation dominates. There are only a few cases (which, as previously mentioned,

are rejected here) where $|A_{AJ}| > \bar{\rho}_{AJ}$. In contrast, the number of occurrences where A_{AJ} is less than zero (i.e., $\rho_{00} < \rho_{12}$) is quite large (ranging from 30 to 55%). In addition, the 0000 and 1200 UTC observations of ρ are not necessarily a good indicator of the diurnal trend of ρ (not shown). Both of these are important issues if one assumes, as AJ do for their hourly

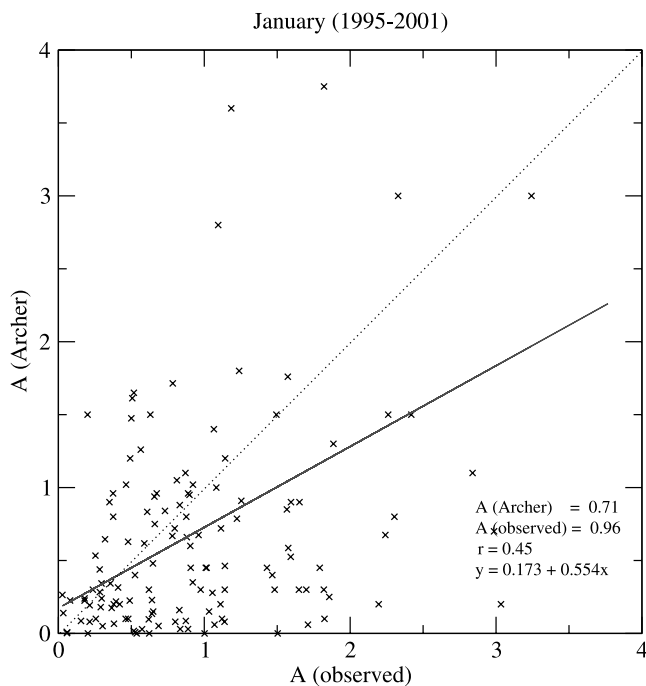


Figure 6. Daily amplitude, A , estimates from AJ (equation (3)) versus the observed A for the month of January (all years). The dotted line is the one-to-one curve, and the solid line is a least squares fit.

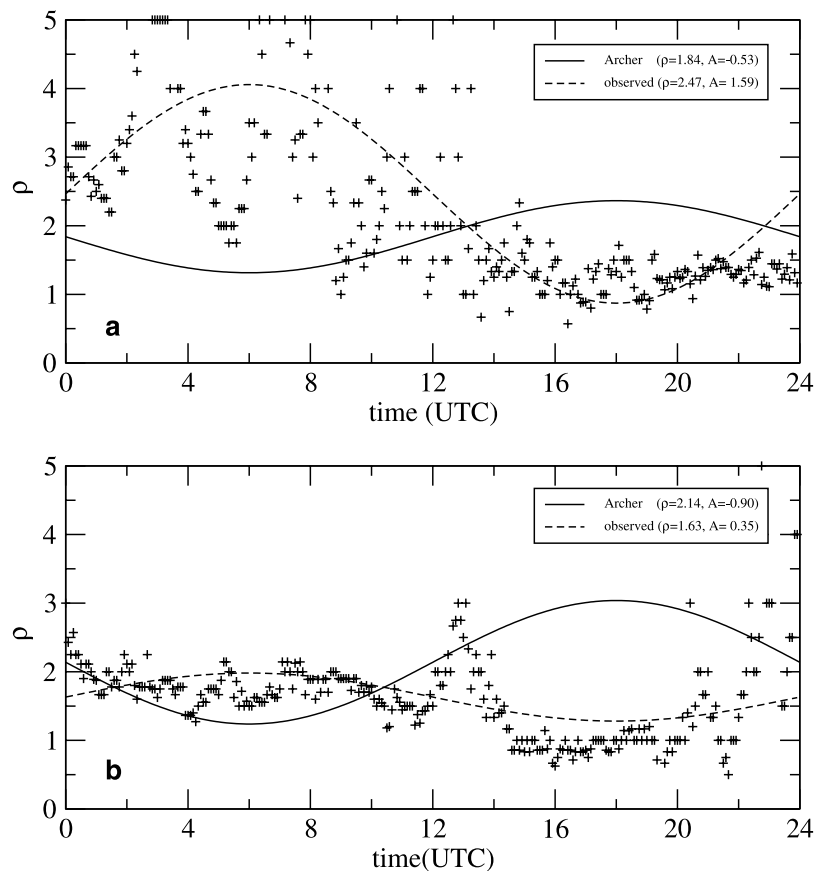


Figure 7. Observed ratio of 80 m to 10 m winds (pluses) for days when the AJ amplitude is negative, (a) 24 January 2000 and (b) 29 January 1996. Least squares sinusoid fit to observations (equation (4)) are shown by the dashed curve, and AJ sinusoid (equation (1)) is shown by the solid curve.

analysis of 10 west/midwest stations, that a negative amplitude indicates a 12 h phase shift in $\rho(h)$. A “12 h phase shift” implies that the sinusoid is multiplied by negative one.

[22] To illustrate the impact of an assumed phase shift for $A < 0$ results are shown for two days where A_{AJ} is less than zero (Figures 7a and 7b). The AJ and least squares sinusoidal fit (equation (4)) are both shown. Clearly, for both of these days, the assumption that the diurnal amplitude is shifted by 12 h is not valid. In fact this assumption alone has a significant impact on the AJ 80 m power estimate for tower 3131. Consider Figure 8 which shows the average observed 10 m winds for January (tower 512 all years (thick solid line) and tower 512 for 2000 (thin solid line)). During the nighttime hours, the 10 m winds are relatively calm and hence the phase of the diurnal signal in ρ will not be as critical when applying equation (5), however during the daytime, the 12 h phase shift results in the AJ ρ maximum coinciding exactly with the maximum in the 10 m winds. The impact of the phase on the wind power can be seen in Figures 9a and 9b, which show the wind power as a function of both ρ and A ($-A$) for a fixed 10 m wind at 1800 UTC (taken to be 4.75 m s^{-1} which is representative of the peak in the 10 m winds shown in Figure 8). Assuming a positive amplitude and taking $\bar{\rho}_{AJ}$ (~ 2.5) and A_{AJ} (0.68) for January (from Table 4) Figure 9a yields a wind power around 400 W m^{-2} (square in Figure 9a). However, for an equivalent negative amplitude (i.e., $A = -0.7$), Figure 9b yields a wind power estimate an order of

magnitude larger (i.e., 2000 W m^{-2} , square in Figure 9b). The wind power for $A < 0$ is shown on Figures 3a and 3b (dashed curves). Both curves are significantly steeper than their positive amplitude counterparts, but more importantly, for $A < 0$ the power actually increases as $|A|$ increases, a direct (and erroneous) result of assuming a 12 h phase shift in ρ (i.e., if the maximum in ρ was instead during the night as observed, an increase in A would act to reduce the average wind power as indicated in Figure 3a). Estimates of A_{AJ} and $\bar{\rho}_{AJ}$ were also calculated separately for cases where $A_{AJ} < 0$ and $A_{AJ} > 0$. The magnitudes of both A_{AJ} and $\bar{\rho}_{AJ}$ for the negative amplitude cases were comparable to the positive amplitude cases (e.g., for the month of January shown here, the negative amplitude cases yield $A_{AJ} = -0.60$ and $\bar{\rho}_{AJ} = 2.32$), indicating that the results presented in Figure 9 are representative of both positive and negative amplitude cases.

[23] To test the hypothesis that power estimate errors using the AJ methodology were a result of an assumed phase shift in ρ , the AJ power is recalculated using the least squares fit of A and $\bar{\rho}$ from equation (4). The parameter, δ , is assumed to be zero and more importantly A is assumed to be positive definite (i.e., $A = |A|$, no phase shifts in ρ). Monthly results, shown in Table 4 (P_{AO}), indicate that the observed fit is quite good and predicts wind power classes that are what one might expect for the region. These results also indicate that a sinusoidal fit is appropriate for this site (assuming no phase shift in ρ and representative values for the AJ parameters). As previously mentioned, removing days

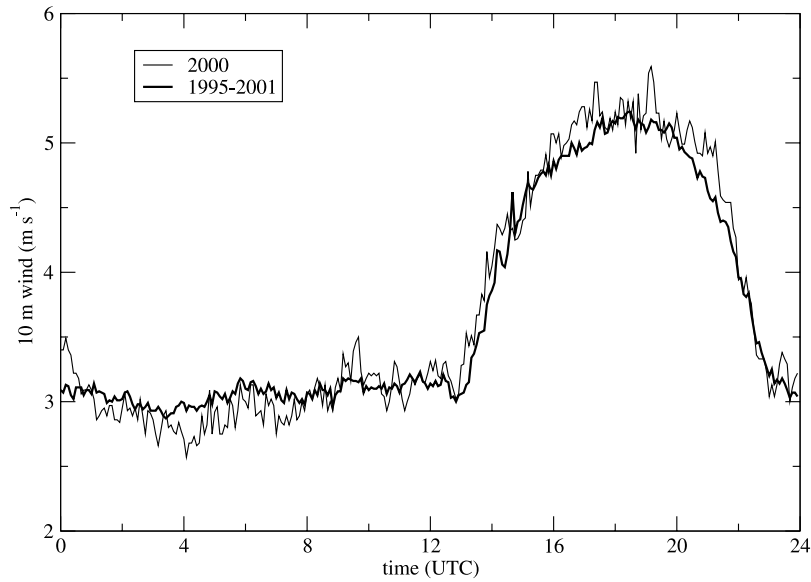


Figure 8. Average observed 10 m (30 feet) wind speed from tower 512 (thick line) for 1995–2001 and tower 512 (thin line) for 2000.

where the amplitude is large, may bias the wind power estimates low by excluding days with significant wind events. However, comparisons with the observed wind power for all days (i.e., including days where the AJ method does not yield an estimate because $|A| > \bar{\rho}$) are also quite good (not shown). Because of this, we do not examine days where $|A| > \bar{\rho}$, however it might be instructive to do so for other stations where significant wind events are more common.

5. Least Squares Evaluation

[24] The AJ least squares (LS) methodology is examined using the data from towers 3131 and 511. To emulate the

AJ method, tower wind profiles are sampled at 0000 and 1200 UTC and then fit independently (via least squares regression) to one of four functions: (1) power law ($V(z_i) = V_R(z_i/z_R)^\alpha$), (2) traditional logarithmic law ($V(z_i) = V_R \ln(z_i/z_o) / \ln(z_R/z_o)$), (3) two-parameter logarithmic law ($V(z_i) = A + B * \ln(z_i)$), and 4.) linear ($V(z_i) = C + D * z_i$), where V_R and z_R are the reference velocity and height, z_i is the observation height, α is the friction coefficient, z_o is the roughness length, and the coefficients A, B, C, D (as defined by the least squares fit) are given in AJ. The tower data used for the regression are measured at 7 fixed levels: 1.8 m, 3.7 m, 9.1 m, 16.5 m, 49.4 m, 62.2 m, 89.9 m, 120.1 m, and 150 m (the reference height is 9.1 m). To be

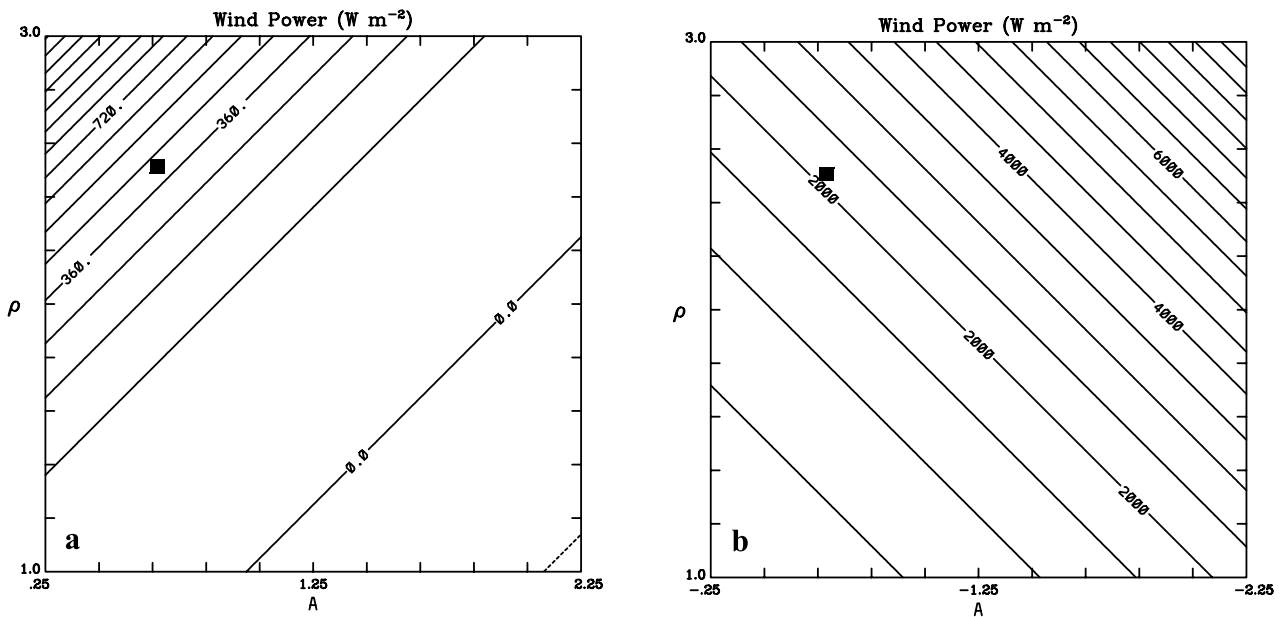


Figure 9. Wind power ($W m^{-2}$, equation (5)) as a function of the AJ inputs, A and $\bar{\rho}$, valid at 1800 UTC and for a 10 m wind speed of $4.75 m s^{-1}$ for (a) $A > 0$ and (b) $A < 0$. Squares denote power estimate using mean January inputs (see text).

Table 5. Monthly Averaged 80 m AJ Least Squares Wind Speed and Wind Power Using the 0000 UTC Tower Winds ($V_{80_{AJ00}}$ and P_{AJ00}) and the 1200 UTC Profiles ($V_{80_{AJ12}}$ and P_{AJ12}), Observed 80 m Wind Speed V_{80} , and Observed Wind Power^a

Month	$V_{80_{AJ00}}$, m s ⁻¹	P_{AJ00} , W m ⁻²	$V_{80_{AJ12}}$, m s ⁻¹	P_{AJ12} , W m ⁻²	V_{80} , m s ⁻¹	P_{V80} , W m ⁻²	P , W m ⁻²	P_f , W m ⁻²
January	7.5	358	6.6	273	6.8	209	254	297
February	7.4	405	7.5	380	6.6	219	265	309
March	7.7	397	7.6	383	6.8	226	273	314
April	7.0	265	6.8	265	6.2	168	203	221
May	5.9	173	5.7	156	5.3	110	134	138
June	5.4	143	4.7	96	4.9	88	112	115
July	4.9	98	4.3	81	4.3	66	84	80
August	5.1	168	4.6	107	4.5	94	120	134
September	5.8	217	4.9	130	5.2	119	146	155
October	7.8	458	6.6	293	6.8	235	268	339
November	7.8	420	6.5	267	6.9	200	236	304
December	6.9	279	6.0	215	6.1	159	191	214

^aThe observed wind power was calculated using (1) the daily average 80 m wind P_{V80} , (2) the 5 min data corresponding to days with regressed profiles P , and (3) the 5 min data with days removed if the friction coefficient is greater than 0.5 or roughness length is greater than 5 m P_f .

consistent with AJ, at least 3 levels must be present at 0000 and 1200 UTC to apply the LS methodology. Although AJ fit 5 proximity soundings, the fit to a single “pseudo” sounding from the tower data, as presented herein, clearly illustrates some of the relevant issues, sensitivities, and problems associated with applying this methodology.

[25] The AJ method estimates the free parameters (i.e., α , z_0 , A, B, C, D in AJ equations (4)–(9)), for the 4 methods, via minimization of the mean square error (i.e., AJ, equation (3)) assuming perfect observations. Using the residual as a metric for the “goodness of fit”, the parameters of the function with the lowest residual are used, along with the daily averaged 10 m wind (for three of the methods), to estimate the 80 m wind. The extrapolation is performed separately for the 0000 and 1200 UTC soundings and then averaged (if they both exist (Archer personal communication, 2004)). The two-parameter log law is employed for cases where the reference velocity (at 0000 or 1200 UTC) is zero while the linear fit is intended for cases where the winds decrease with height. However, it is worth pointing out that the two-parameter log fit will often yield a lower residual than the traditional log law but does so at the expense of removing the horizontal variability represented by the 10 m wind.

[26] Table 5 lists the monthly averaged 80 m wind and power estimates obtained from the AJ LS methodology using the 0000 UTC profiles ($V_{80_{AJ00}}$ and P_{AJ00} respectively) and 1200 UTC profiles ($V_{80_{AJ12}}$ and P_{AJ12} respectively). Table 5 also contains the observed 80 m wind power estimated using the daily mean 80 m wind as input (P_{V80}); the 5 min. data for days when a regressed profile exists (P); and the 5 min. data when a regressed profile exists but with days removed where the friction coefficient or roughness exceeds 0.5 and 5 respectively (P_f). To be consistent with the AJ method, a daily average is first produced from which an average for the month is obtained. The removal of observations for days (profiles) in which a regression (i.e., LS fit) does not exist and for cases where the friction coefficient α exceeds 0.5 or the roughness length z_0 is greater than 5 m, produces a high bias in both V_{80} and P_f (i.e., larger than their “true” estimates) for most months (compare V_{80} and P in Tables 4 and 5).

[27] For all months, $V_{80_{AJ00}}$ is greater than the observed 80 m winds. Regression results based on the 1200 UTC profiles indicate that $V_{80_{AJ12}}$ are less than $V_{80_{AJ00}}$ for all

months and less than the observed 80 m winds for September–January and June. The LS methodology yields, for the 0000 UTC wind profiles, class 3 and 4 wind power estimates for October through April, a departure from the observed wind power class of 2 for these months. Differences in the LS average daily power for the two profiles approach 150 W m⁻² (October/November) with power estimates being larger for all months for the 0000 UTC extrapolation. The differences between the two profile estimates are associated, in part, with boundary layer decoupling which contributes to a decreased 10 m wind for the 1200 UTC profiles. AJ power estimates are larger than observed for all months for the 00 UTC profiles and larger than observed for all but the summer months (June–September) for the 12 UTC profiles.

[28] Differences between the observed daily-averaged power and the LS methodology in excess of 500 W m⁻² are identified in Table 6 (% flagged profiles). Here, cases where the friction coefficient α exceeds 0.5 or the roughness length z_0 is greater than 5 m have been included in order to illustrate the impact of these two fitting parameters on the regression. A considerable number of profiles yield AJ power estimates that differ (from the observed) by

Table 6. Percentage of Flagged Profiles for Cases Where the AJ Power is More Than 500 W m⁻² Greater Than Observed, Percentage of Flagged Power Law Profiles Where the Friction Coefficient α is Greater Than 0.5, and the Observed 10 m (\bar{V}_{10}) (Daily) Mean Wind Minus the 0000 and 1200 UTC 10 m (V_{10}) Winds

	Flagged, %		$\alpha > 0.5$, %		$\bar{V}_{10} - V_{10}$, m s ⁻¹	
	0000	1200	0000	1200	0000	1200
January	19.9	20.6	77.8	76.9	0.69	0.68
February	17.6	21.4	55.6	75.0	0.42	0.41
March	11.5	23.9	33.3	62.9	0.35	0.31
April	6.3	20.6	44.4	72.0	0.19	0.18
May	5.2	5.6	50.0	75.0	-0.10	-0.09
June	3.7	3.2	60.0	100.0	-0.15	-0.14
July	0.6	3.3	100.0	100.0	-0.26	-0.27
August	1.7	8.6	0.0	88.9	-0.04	-0.04
September	5.5	12.0	50.0	83.3	0.20	0.23
October	15.7	14.7	45.5	66.7	0.42	0.43
November	20.0	17.0	61.1	85.7	0.52	0.55
December	17.3	12.5	80.0	78.6	0.44	0.47

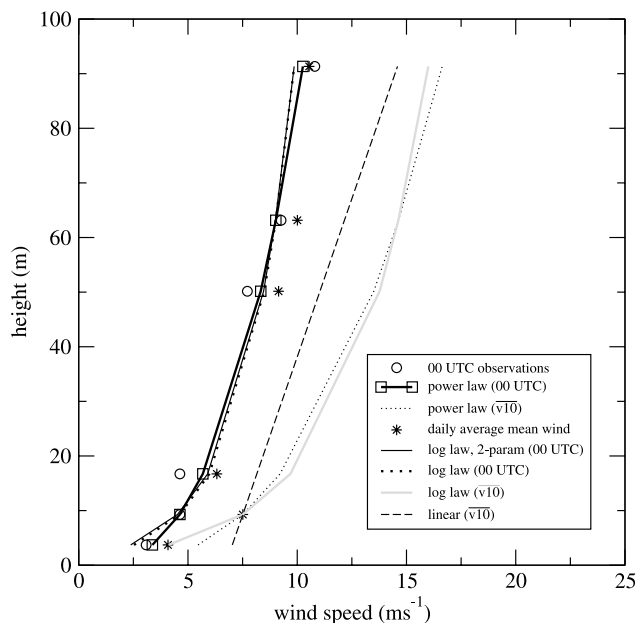


Figure 10. Least squares fit to a 0000 UTC 23 February 1998 observed wind profile (open circles). The power law (lowest residual) is given by the thick solid line and squares, the two-parameter log fit is given by the thin solid line, and the traditional log law fit is given by the thick dotted line. The observed mean wind profile for the day (asterisk) and the associated power law fit (thin dotted line), log law fit (solid shaded line), and linear fit (dashed line) are also shown.

more than 500 W m^{-2} , ranging from a maximum of 23.9% (1200 UTC, March) to less than 1% (0000 UTC, July). The percentage of the total number of “rejected” power law profiles for which the friction coefficient α exceeds 0.5 is given in Table 6 ($\alpha > 0.5$). The power law is emphasized here because it yields the lowest residual on the order of 15 to 20% of the time, but is responsible for a disproportionate number of the total flagged profiles when compared to the other methods and yields the largest overall biases for all months and both profiles (not shown). A significant percentage (greater than 40%) of “flagged” power law profiles would not be removed from the analysis during the region’s significant wind months (i.e., October–March). Although the removal of large friction coefficient profiles improves the 80 m wind estimates (not shown), the AJ power estimates still exceed the observed for all but the 1200 UTC profiles for June–September (Table 5).

[29] As mentioned, not all of the spurious (flagged) power law profiles are rejected however (i.e., a relatively significant number of rejected profiles actually have values of $\alpha < 0.5$). A comparison of the November statistics for which there is a large difference between the 0000 and 1200 UTC power estimates (420 W m^{-2} versus 267 W m^{-2} , Table 5) nicely illustrates the impact of the rejection as only 61% of the flagged power law profiles are removed from the 0000 UTC power estimate versus 86% for the 1200 UTC profile. At this site, a smaller cutoff value for the power law coefficient α would improve power estimates by removing more of the offending profiles. However, to do so would further reduce the amount of data (which, for some of the

site’s relatively significant wind months, is already reduced on the order of 20%).

[30] Figure 10 represents a “flagged” (i.e., a bias $> 500 \text{ W m}^{-2}$ in the estimated power) 23 February 1998 0000 UTC profile, for which the power law ($\alpha = 0.35$) is the lowest residual method. Figure 10 illustrates why it can be problematic to couple a daily mean 10 m wind with a profile fit at 0000 or 1200 UTC. For this case, the 10 m mean wind is approximately 2 m s^{-1} greater than its 0000 UTC counterpart. Under these circumstances, any of the least squares fit methods at the times of 0000 and 1200 UTC are generally superior (i.e., more representative of the average daily power) to an extrapolation method that uses the fit at these times in combination with the daily-averaged 10 m mean wind. For this case (and others not shown here) spuriously large 80 m wind estimates will occur for any of the methods when their LS parameters are applied to the daily-averaged 10 m wind. While the observed 0000 UTC 80 m wind (open circles) is representative of the observed 80 m mean wind for the day (asterisks), the 0000 UTC 10 m wind is significantly smaller than its daily mean.

[31] The observed 80 m winds are compared to their LS counterparts for 0000 UTC, February 1995–2001 cases (Figure 11, with cases where the friction coefficient α exceeds 0.5 or the roughness length z_0 is greater than 5 m removed). As previously mentioned, most of the high biased 80 m wind estimates are associated with the power law, with all but a few power law estimates yielding 80 m winds greater than the observed (see Figure 11). For values of the 10 m wind on the order of $5\text{--}6 \text{ m s}^{-1}$ (comparable to the observed winds at this site), 80 m wind estimates obtained via the power law will vary by 1 to 3 m s^{-1} for

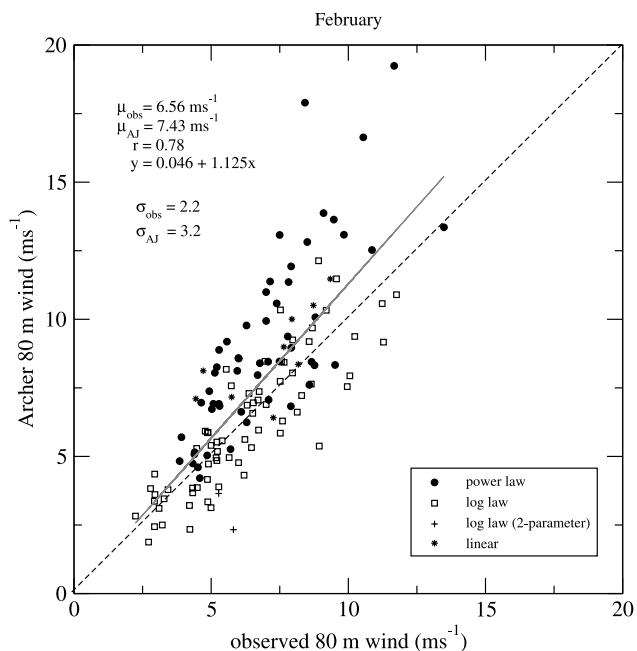


Figure 11. Observed versus AJ 80 m winds from a least squares fit for 1995–2001 February 0000 UTC profiles. Each point represents the method with the lowest residual: the power law (circles), log law (squares), two-parameter log law (pluses), and linear (asterisks). The dashed line is the one-to-one curve, and the solid line is a least squares fit.

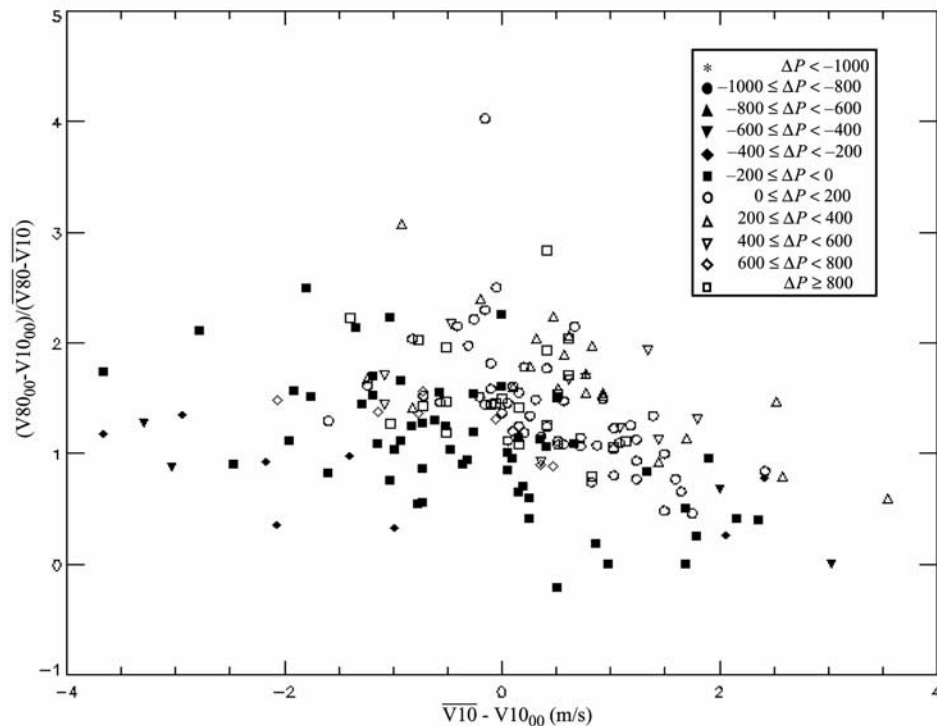


Figure 12. February 1995–2001 regressed/observed power difference (W m^{-2}) ΔP ($P_{AJ} - P$) as a function of the difference between the 10 m daily-averaged and 0000 UTC wind (abscissa) and the difference ratio between the 80 m and 10 m 0000 UTC and mean winds (ordinate), respectively.

values of the friction coefficient ranging from 0 to 0.5. Obviously, under the appropriate circumstances this is a desired result (i.e., representative of the true vertical wind profile). However, for this site, the 10 m mean winds are “biased high” (i.e., greater than the profile winds) for both profiles (0000 and 1200 UTC) and all months with the exception of summer (May–August, Table 6).

[32] In an effort to quantify the high bias in the AJ 80 m wind, the regressed minus observed power difference (ΔP , W m^{-2}) is plotted as a function of the difference between the 10 m daily-averaged and 0000 UTC wind ($\overline{V10} - V10 \text{ m s}^{-1}$, abscissa), and the difference ratio between the 80 m and 10 m 0000 UTC and mean winds respectively ($(\overline{V80_{00}} - V10_{00})/(\overline{V80} - \overline{V10})$, ordinate) for February 1995–2001 (Figure 12). The difference ratio is a measure of the relative slope of the 0000 UTC wind profile to that of the mean profile while the abscissa represents the difference between the intercepts for the 0000 UTC and the mean wind profile. For zero intercept difference, a difference ratio greater (less) than one will trend toward a high (low) power estimate for a given day. Similarly, for a fixed difference ratio of one, a positive (negative) intercept will tend to produce power estimates greater (less) than observed. Figure 12 shows a relatively clear delineation between the positive and negative power bias, with increasing positive bias (i.e., $P_{AJ} > P$) for both larger intercept and slope differences. Figure 12 also indicates that the negative bias is generally low ($<200 \text{ W m}^{-2}$, solid squares). In tandem, the slope and intercept biases are a good predictor of the performance of the AJ LS methodology. Additionally, the monthly average intercept bias alone is also a good indicator of the AJ method performance (see Table 6) with negative/

low intercept bias during May–August (power estimates within 50 W m^{-2} of the observed) and positive/high intercept bias during October–March (power estimates on the order of 100 W m^{-2} larger than observed).

6. Conclusions

[33] Both the temporal and spatial aspects of the wind power parameterization of Archer and Jacobson are examined using a combination winds from 4 towers in the Kennedy Space Center/Canaveral Air Force Station tower network. Various sensitivities in the temporal and spatial extrapolation methods are exposed, the latter of which may explain, to some extent, the high degree of variability and ostensibly spurious AJ wind power estimates along the central east Florida coast. With respect to the temporal component of the AJ parameterization, the findings include the following.

[34] 1. AJ estimates of the ratio of the 80 m to 10 m winds are robust but biased high. The relatively good estimates of this ratio indicate that the temporal variation of the observations can be approximated by a sinusoid (with the high bias related to the fact that the observed time series is not a “pure” sinusoid).

[35] 2. Observed and parameterized diurnal amplitude of the ratio of the 80 m to 10 m winds are poorly correlated because the estimate of the assumed sinusoidal amplitude uses only two points and is thus sensitive to small phase shifts in the diurnal signal.

[36] 3. For this site it is incorrect to assume that negative amplitude estimates from equation (3) are indicative of a true diurnal phase shift in the ratio of the 80 m to 10 m winds.

[37] 4. The parameterized and observed power are in good agreement if (1) there are no assumed phase shifts in the diurnal time series of 80 m to 10 m wind ratio and (2) the best fit parameters from the observations (for that day) are used as inputs.

[38] 5. This site may not be an appropriate site for evaluating the hourly methodology, given the time zone of Florida (4–5 hours from UTC) as the sounding times often produce small and/or negative amplitude estimates.

[39] An examination of the spatial component of the AJ parameterization, which involves a least squares fit (to one of four assumed wind profiles) using 0000 and 1200 UTC tower winds, indicates the following.

[40] 1. The power law, which frequently yields the lowest residual (on the order of 15 to 20% of the time), is responsible for a disproportionate number of profiles (when compared to the other LS methods) with power estimates greater than observed.

[41] 2. For this site the daily-averaged 10 m wind is often larger than both the 0000 and 1200 UTC 10 m winds for all months with the exception of summer (May–August). Months for which the AJ methodology performs well (May–August) are correlated with negative/low bias (i.e., the daily average 10 m mean wind is comparable to the 0000 and 1200 UTC 10 m winds), while months where it is degraded (October–March) are associated with positive/high bias (i.e., the daily average 10 m mean wind is larger than the 0000 and/or 1200 UTC 10 m winds). Power bias estimates (i.e., AJ minus observed) indicate that the 0000 and 1200 UTC profiles are often not representative of the observed mean wind profile and combine (with the 10 m wind bias) in such a way as to systematically produce a high bias in the monthly LS power estimates.

[42] **Acknowledgment.** The authors would like to thank W. Lambert and J. Case of ENSCO Inc./Applied Meteorology Unit contract for

providing the wind tower data, Frank Leslie, Florida Institute of Technology, for providing invaluable feedback, and Christina Archer, Stanford University for her feedback, comments and correspondence.

References

- Archer, C. L., and M. Z. Jacobson (2003), The spatial and temporal distributions of U.S. winds and wind power at 80 m derived from measurements, *J. Geophys. Res.*, 108(D9), 4289, doi:10.1029/2002JD002076.
- Arya, S. P. (1988), *Introduction to Micrometeorology*, 307 pp., Elsevier, New York.
- Brower, M. (2002), Wind resource maps of southern New England, project report, 14 pp., Conn. Clean Energy Fund, Rocky Hill.
- Elliott, D. L., C. G. Holladay, W. R. Barchet, H. P. Foote, and W. F. Sandusky (1986), *Wind Energy Resource Atlas of the United States*, Natl. Renewable Energy Lab., Golden, Colo.
- Lambert, W. (2002), Statistical short-range guidance for peak wind speed forecasts on Kennedy Space Center/Cape Canaveral Air Force Station: Phase 1 results, *Rep. NASA/CR-2002-211180*, 33 pp., Appl. Meteorol. Unit, Kennedy Space Cent., Cape Canaveral, Fla.
- Larson, V. E., R. Wood, P. R. Field, J.-C. Golaz, T. H. Vonder Haar, and W. R. Cotton (2001), Systematic biases in the microphysics and thermodynamics of numerical models that ignore subgrid-scale variability, *J. Atmos. Sci.*, 58, 1117–1128.
- Petersen, E. L., I. Troen, S. Frandsen, and K. Hedegard (1981), Windatlas for Denmark. A rational method for wind energy siting, *Rep. Risø-R-428*, Risø Natl. Lab., Roskilde, Denmark.
- Sandusky, W. F., D. S. Renne, and D. L. Hadley (1982), Candidate wind turbine generator site summarized meteorological data for the period December 1976 to December 1981, *Rep. PNL-4407*, Pac. Northwest Lab., Richland, Wash.
- Schwartz, M., and D. Elliot (2001), Remapping of the wind energy resource in the midwestern United States, *Rep. NREL/AB-500-31083*, Natl. Renewable Energy Lab., Golden, Colo.
- Troen, I., and E. L. Petersen (1989), *European Wind Atlas*, 656 pp., Risø Natl. Lab., Roskilde, Denmark.
- Wessel, P., and W. H. F. Smith (1995), New version of the Generic Mapping Tools released, *Eos Trans. AGU*, 76, 329.

J. Bewley and S. M. Lazarus, Department of Marine and Environmental Systems, Florida Institute of Technology, 150 West University Boulevard, Melbourne, FL 32901, USA. (slazarus@fit.edu)